Romanian Reports in Physics **72**, 601 (2020)

NOVEL BIO-FRIENDLY NANOMATERIALS BASED ON ARTIFICIAL CELL MEMBRANES, CHITOSAN AND SILVER NANOPARTICLES PHYTOGENERATED FROM *EUGENIA CARYOPHYLLATA* BUDS: ECO-SYNTHESIS, CHARACTERIZATION AND EVALUATION OF BIOACTIVITIES

M. E. BARBINTA-PATRASCU[1], N. BADEA[2], MIHAELA BACALUM[3], S. ANTOHE[1,4*]

[1] University of Bucharest, Faculty of Physics, Department of Electricity, Solid-State Physics and Biophysics, 405 Atomistilor Street, PO Box MG-11, Bucharest-Magurele, 077125, Romania
E-mail: *elipatras@gmail.com*, *santohe@solid.fizica.unibuc.ro*
[2] "Politehnica" University of Bucharest, Faculty of Applied Chemistry and Materials Science 1–7, Polizu Str., 011061, Bucharest, Romania
Email: *nicoleta.badea@gmail.com*
[3] "Horia Hulubei" National Institute for Physics and Nuclear Engineering, Department of Life and Environmental Physics, Reactorului 30, PO Box MG-6, Măgurele 077125, Romania
Email: *bmihaela@nipne.ro*
[4] Academy of Romanian Scientists, 54 Splaiul Independentei, Bucharest, Romania
Email: *s_antohe@yahoo.com*
[*] Corresponding author: *santohe@solid.fizica.unibuc.ro, s_antohe@yahoo.com*

Received November 7, 2019

Abstract. This paper reports a creative *bottom*-up eco-benign design of novel nanocomposites based on bio-inspired membranes, *green* nanosilver and chitosan, for biomedical purposes. Chlorophyll *a* was used as a sensor to monitor the nanomaterial biofabrication, by UV-Vis absorption and fluorescence emission spectroscopy. SEM analysis confirmed the phytosynthesis of AgNPs (from *Eugenia caryophyllata* aqueous extract), and the formation of silver-based materials. The developed nanomaterials presented hemocompatibility, high antioxidant activity (90.2÷99.1%, checked by chemiluminescence method), anti-proliferative effect against HT-29 cancer cells, and no toxicity to normal cells in a dose-dependent manner. Chitosan and biomimetic membranes induced biocompatibility and interesting bio-activities of the obtained materials.

Key words: phytogenic silver-based nanomaterials, chlorophyll-labelled artificial cell membranes, antiproliferative activity.

1. INTRODUCTION

Nowadays there is a great trend to reuse and recycling vegetal wastes, in order to keep clean the environment and to reduce the costs. From environmental perspective, the "green" nanotechnologies offer safer approaches to keep clean the environment. In this respect, natural raws were used in this study to obtain novel biohybrids based on biomimetic membranes, *green* nanosilver and chitosan, for antioxidant and antiproliferative activity, as adjuvants in colon cancer therapy.

The biofabrication of metal nanoparticles (MNPs) using vegetal extracts, is an environment-friendly, safe, rapid and cost-effective procedure, avoiding the use of toxic chemicals. The resulting MNPs are "wrapped" by phytochemicals which confer interesting biological activities like: biocompatibility, antioxidant properties and anti-proliferative activity [1–4]. Some *et al*. highlighted the crucial role played by several plant metabolites (like polyphenols, sugars, terpenoids, alkaloids, proteins and phenolic acids) in the bio-reduction of silver ions [5]. On the other hands, metal particles within the *nano* size possess features those are quite distinct from both the ion and the bulk material [6] offering very interesting properties of great significance in various fields. An interesting nano-metal is nano-silver which is cheap and has unique properties; the silver nanoparticles (AgNPs) are widely used in biomedicine [7], photovoltaic devices [8], or cosmetics [9]. Moreover, the biogenerated nano-silver by using vegetal extracts are exciting materials with huge potential in bio-applications [4, 10–11] or as biopesticides [12].

The aim of this study was to design novel bio-friendly architectures based on artificial cell membranes, chitosan and "green" silver nanoparticles with good bioperformances. The aromatic precious spice *Eugenia caryophyllata* L. was chose to bio-generate silver nanoparticles, due to its bio-composition rich in biomolecules (flavonoids, phenolic acids and essential oils) that have antioxidant and anticarcinogenic activities [10, 13–14]. The presence of biomimetic systems based on dipalmitoyl phosphatidylcholine (DPPC) will improve the bioavailability and the biocompatibility of the metal-based biocomposites, as previously demonstrated by Barbinta-Patrascu *et al*. [10, 15] which developed biohybrids containing soybean-lecithin liposomes and silver nanoparticles with low toxicity on normal cells and anti-proliferative activity on HT-29 human colorectal cancer cells. In this research study, the liposomes based on DPPC containing nanosilver were self-assembled with chitosan-coated artificial cell membranes. Chitosan (CS) is an interesting cationic polysaccharide, a linear copolymer of glucosamine and N-acetylglucosamine units linked by β-(1–4) glycosidic linkages [16], often used in biomedical field due to its broad spectrum of properties: biodegradability, biocompatibility, non-toxicity, non-antigenicity, bio-adhesivity, antimicrobial & biological activity, with a hemostatic effect [17]. The bio-fabricated silver-based materials in this research work, were characterized by UV-Vis absorption and fluorescence emission spectroscopy, zeta potential measurements and SEM analysis. Their biological value was tested by evaluating the antioxidant properties, the cytotoxic effects on L929 normal cells, and the antiproliferative effect on HT-29 human colorectal cancer cells.

2. MATERIALS AND METHODS

2.1. MATERIALS

KH_2PO_4, Na_2HPO_4, Tris (hydroxymethylaminomethane base), HCl, H_2O_2, luminol (5-amino-2,3-dihydro-phthalazine-1,4-dione), glacial acetic acid, were

purchased from Merck (Germany). Silver nitrate was acquired from Gatt Koller – GmbH Austria. Dipalmitoyl phosphatidylcholine (DPPC), Drabkin reagent, standard hemoglobin, acridine orange (AO), ethidium homodimer-1 (EthD-1), NaCl and chitosan (CS, from crab shells, highly viscous, ≥ 85% deacetylated) were supplied by Sigma Aldrich (Germany). Chlorophyll *a* was isolated from fresh leaves of *Spinacia oleracea* L. as described in [18]. The dried flower buds of *Eugenia caryophyllata* were acquired from a local market. L929 mouse fibroblast cells and HT-29 human colorectal adenocarcinoma cells (ATCC, USA) were grown in MEM (Mimimal Essential Medium) and DMEM (Dulbecco's Modified Eagle Medium) respectively, supplemented with 10% fetal calf serum (FCS), 2 mM L-Glutamine, 100 units/ml of penicillin and 100 μg/ml of streptomycin at 37°C in a humidified incubator under an atmosphere containing 5% CO_2. All cell cultivation media and reagents were purchased from Biochrom AG (Berlin, Germany).

2.2. SAMPLE PREPARATION

Preparation of silver nanoparticles (AgNPs). The phytogenic silver nanoparticles (AgNPs) were prepared according to the "green" method described in [19–20]. Briefly, an amount of 30 g of cleaned dry flowers of *Eugenia caryophyllata* L. were finely ground and then mixed with 150 ml hot distilled water and boiled for 10 minutes in order to release the intracellular phytoactive compounds into solution. This mixture was then cooled and filtered through a Wathman no.1 filter paper resulting in a clear extract. An appropriate volume of this aqueous as-prepared extract was mixed with an equal volume of 1 mM $AgNO_3$ aqueous solution, under rigorous stirring at room temperature, for 24 h. The change of mixture color from dark yellowish to dark brown indicates the formation of AgNPs. The process of bioreduction of Ag^+ arising from $AgNO_3$ aqueous solution, by the bioconstituents of the *Eugenia caryophyllata* extract, can be summarized by the following equation:

$$Ag^+ + \text{phyto-molecules (from plant extract)} \rightarrow \text{AgNPs}. \quad (1)$$

The chlorophyll-labelled liposomes (Lip) were obtained by the procedure described by Barbinta-Patrascu *et al.* [21]. Thus, multilamellar lipid vesicles (MLVs, 0.5 mM) were obtained by hydration of a thin film consisting of a mixture of DPPC and Chl*a* in a molar ratio of 100:1, with a solution of phosphate buffer saline Na_2HPO_4–KH_2PO_4–NaCl (PBS) at physiological pH (7.4). Chlorophyll *a*, a natural porphyrin, the key molecule in the photosynthesis process was previously reported as a spectral marker for monitorization the formation of silver-based nanomaterials [4, 14, 15, 19].

Preparation of liposomes/AgNPs biocomposites (BC1). Biomaterials based on artificial lipid membranes and phytogenic AgNPs (biocomposites BC1) were obtained by subjecting a mixture of liposomes and AgNPs (in a volumetric ratio of 1:1) to an ultrasound-assisted method (5 minutes; Hielser Ti probe sonicator, UP 100 H).

Preparation of liposomes/AgNPs/chitosan biocomposites (BC2). The biocomposites BC2 containing liposomes, AgNPs and chitosan, were obtained by self–assembling

a mixture of BC1 and chitosan (CS) 1% (w/v in acetic acid solution 0.4% v/v), in a volumetric ratio BC1:CS = 10:1. This mixture was then strong stirred (VIBRAX stirrer – Milian USA, OHIO 43230 USA 200 rpm) for 15 min.

The experiments were carried out in dark to prevent the photodegradation of the obtained specimens. A summary of the samples' abbreviations is displayed in Table 1. A schematic representation of the preparation of the silver-based materials is described in Fig. 1.

Table 1

The abbreviations of the samples

Sample	Code
Chitosan	CS
AgNPs phytogenerated from *Eugenia caryophyllata*	AgNPs
Chl*a*-DPPC Liposomes	Lip
Chl*a*-DPPC Liposomes/AgNPs chitosan biocomposites	BC1
Chl*a*-DPPC Liposomes/AgNPs/ chitosan biocomposites	BC2

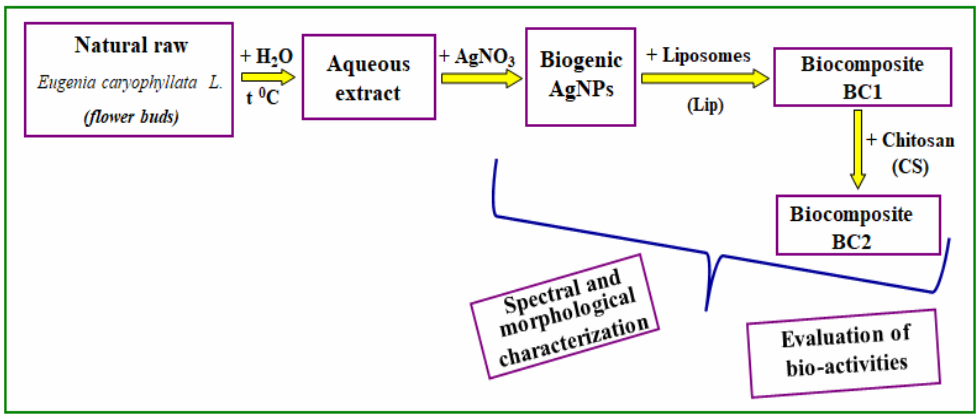

Fig. 1 – "Green" preparation schema of the silver-based materials from *Eugenia caryophyllata* L.

2.3. CHARACTERIZATION METHODS

A double beam Lambda 2S Perkin Elmer UV-Vis spectrophotometer, operated at 1 nm resolution, was used to record the **UV-Vis absorption spectra** in the 400–800 nm wavelength range.

Fluorescence emission spectra of Chl*a* in samples were recorded in the wavelength range of 600–800 nm, on a LS55 Perkin Elmer fluorescence spectrometer, by illuminating the samples with 430 nm excitation light.

Zeta potential (ξ) values were measured in triplicate, using a special dispositive of Zetasizer Nano ZS (Malvern Instruments Ltd., UK) by applying an electric field across the analyzed aqueous samples.

SEM analysis was performed on FEI Inspect S Scanning Electron Microscope (SEM) working under up to 30 kV acceleration voltage.

A luminol-based free radical generator system (containing 10^{-3} M luminol, 10^{-5} M H_2O_2, in TRIS-HCl buffer solution pH 8.6) was used for ***in vitro* assessment of antioxidant power** of the samples by **chemiluminescence method**. These investigations were performed on a Chemiluminometer Turner Design TD 20/20 (USA), and the values of *in vitro* antioxidant activity (AA%) of the samples was quantified by the equation:

$$\mathrm{AA} = [(I_0 - I) / I_0] \cdot 100\ [\%] \tag{2}$$

where I_0 is the maximum CL intensity at t = 5 s, for the reaction mixture without the sample, and I is the maximum CL intensity for each sample at t = 5 s [22]. Three different experiments were carried out for each sample.

The *in vitro* cytotoxicity was assessed by CellTiter 96 AQueous One Solution Cell Proliferation Assay kit (Promega, Madison, WI, USA) following the instruction from the manufacturer. Briefly, the appropriate amount of cells (L929: 8000 cells/well and HT-29 cells: 16000 cells/well) were seeded in 96 well plates and grown for 24 h in medium. After 24 h, the old medium was replaced by fresh medium containing different concentrations of hybrid. Untreated cells were used as negative control. After a 24 h treatment, the medium was changed and 20 µl of MTS solution was added in each well and incubated at 37°C for additional 4 h. The absorbance was recorded at 490 nm using a microplate reader (Mithras 940, Berthold, Germany). The data were corrected for the background and then the percentage of viable cells was calculated according to the following equation:

$$\text{Viable cells} = A_p / A_o\ [\%] \tag{3}$$

where: A_p is the absorbance at 490 nm for the cells treated with different concentrations of samples, and A_o is the absorbance of the untreated cells.

The concentration at which the cellular growth was inhibited by 50% (IC_{50}) was obtained by fitting the survival curves with a sigmoid function.

The haemolytic activity of each sample was determined using an adapted protocol based on the ASTM F 756-00 standard described previously [23–24]. The blood was collected from healthy volunteers and diluted with PBS to a final concentration of haemoglobin ~10 mg/ml. The blood was incubated for 4 h at 37°C with the highest concentration of the tested samples. After 4 h, the cells were centrifuged at 800 g, the supernatant collected, transferred into 96-well tissue culture plates and mixed with an equal amount of Drabkin reagent. After 15 minutes the absorbance of the samples was read at 570 nm using a plate reader. As negative and positive controls, we used human red blood cells (hRBCs) in PBS and distilled water, respectively. The values obtained were corrected for the background, dilution factors and used to calculate the % haemolysis (haemolytic index) according to the following equation:

$$\text{Haemolysis} = A^{SB} / A^{TB} \cdot 100\ [\%] \quad (4)$$

where: A^{SB} is the corrected absorbance of the haemoglobin released in supernatant after treatment with hybrids, and A^{TB} is the corrected absorbance of the total haemoglobin released.

3. RESULTS AND DISCUSSIONS

3.1. CHARACTERIZATION OF THE OBTAINED NANO-METALLIC PARTICLES

The biosynthesis of AgNPs was observed by a visually inspection of the colour modification of the mixture: phyto-extract + 1mM $AgNO_3$ *solution*; the colour turned from yellowish red to dark brown with mirror-like illumination (see Fig. 2, *Inset*). The aqueous extract of *Eugenia caryophyllata* buds acted both as a bioreducing and capping agent to generate AgNPs.

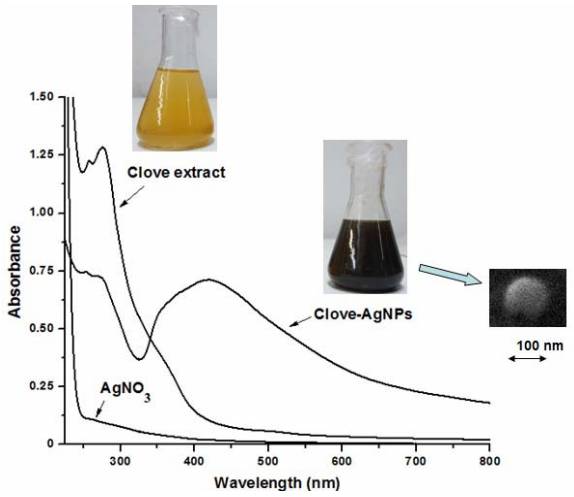

Fig. 2 – The comparative absorption spectra of *Eugenia caryophyllata* extract, phytogenic AgNPs and 1mM $AgNO_3$ solution (recorded in distilled water). *Inset*: The flasks containing phyto-extract and AgNPs, and also the SEM image of the obtained AgNPs.

The phyto-mediated synthesis of silver nanoparticles was monitored by UV-Vis absorption spectroscopy (Fig. 2). The UV-Vis absorption spectrum of AgNPs bio-generated from *Eugenia caryophyllata*, showed a strong single nearness SPR peak located at 420 nm wavelength, observed after addition of 1mM $AgNO_3$ solution to the phyto-extract, highlighting the formation of bio-nanosilver. It must be noted that this peak is not present in the clove extract. The occurring of only one SPR band is characteristic for silver nanoparticles spherical in shape [25]. These

morphological aspects were confirmed by SEM image (Fig. 2, *Inset*) which shows the nano-scaled size of the obtained AgNPs.

3.2. OPTICAL CHARACTERIZATION OF BIOSILVER – CONTAINING MATERIALS

UV-Vis absorption and fluorescence emission spectroscopy were used to demonstrate the formation of biosilver – containing materials labelled with chlorophyll as an optical sensor. Figure 3 displays the absorption spectra (normalized at 800 nm) of the bio-based hybrids BC1 and BC2, as compared to their *building blocks*: Lip, phytogenic AgNPs and chitosan, in physiological conditions (PBS pH 7.4). These spectra highlights the spectral signatures of Chl*a* and of AgNPs, suggesting the incorporation of Chl*a* and AgNPs in the two bio-colloidal materials BC1 and BC2. The presence of spectral fingerprint of AgNPs in biohybrids is noticed by a red shifting of AgNPs SPR band from 469 nm (recorded in PBS) to 507 nm in BC1, and to 500 nm in BC2. On the other hand, the main spectral signature of Chl*a* at 672 nm in liposomes Lip slightly blue shifted to 671 nm in BC1, and to 669 nm in BC2. These shifts confirm the synthesis of bionanosilver – containing hybrid materials, and also the role of Chl*a* in sensing this process.

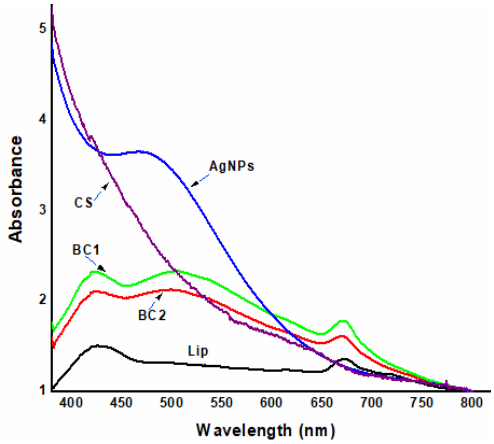

Fig. 3 – The absorption spectra (normalized at 800 nm) of the hybrids BC1 (3) and BC2, obtained from liposomes Lip, phyto-generated AgNPs and chitosan, in PBS pH 7.4. The Chl*a*-based samples (Lip, BC1 and BC2) were corrected against light scattering as described in [26].

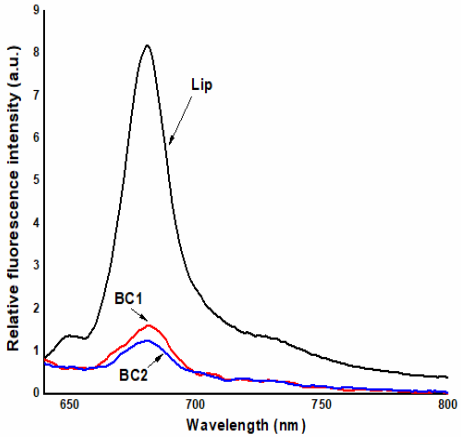

Fig. 4 – The emission spectra of the Chl*a*-labelled materials, in PBS pH 7.4. The excitation wavelength was 430 nm.

The bio-fabrication of biohybrids BC1 and BC2 was further evidenced by fluorescence emission spectra, under excitation wavelength of 430 nm (Fig. 4). The spectral fingerprint of Chl*a* in Chl*a*-labelled materials was observed at 681 nm. The Chl*a* fluorescence intensity of liposomes Lip decreased by 80.24% after addition of AgNPs to liposomes (see sample BC1 in Fig. 4).

A fluorescence quenching effect (22.37%) was also observed after chitosan addition to BC1, when result in the biocomposite BC2 (Fig. 4). This fluorescence quenching effects are due to the electron-transfer process when the chromophore of Chl*a* (the porphyrinic ring) is in close proximity to the surface of silver nanoparticles to donate the excited electrons to the metal nanoparticles [27–28].

3.3. EVALUATION OF PHYSICAL STABILITY OF BIO-COLLOIDAL MATERIALS

The physical stability of the samples was estimated experimentally, based on electrophoretic mobility, in terms of zeta potential, ξ (see Fig. 5) as an indicator of the stability of colloidal systems [29]. In addition, ξ is related to the surface charge of particles. The liposomes alone (ξ = –17.2 mV) and the phytosynthesized AgNPs (ξ = –19.4 mV) exhibited short-term stability assured by repulsive forces. The liposomes/AgNPs biocomposites (BC1) presented good stability (ξ = –28.97 mV) through interparticle repulsion. The negative surface charge of BC1 was adequate for coating them with the positively charged chitosan (ξ = +3.92 mV), resulting in BC2 biocomposite beads with positive ξ value (+13 mV). This shift of Zeta potential values from negative value (BC1) to positive ones (BC2) confirms the presence of the chitosan coat on BC2 sample [15].

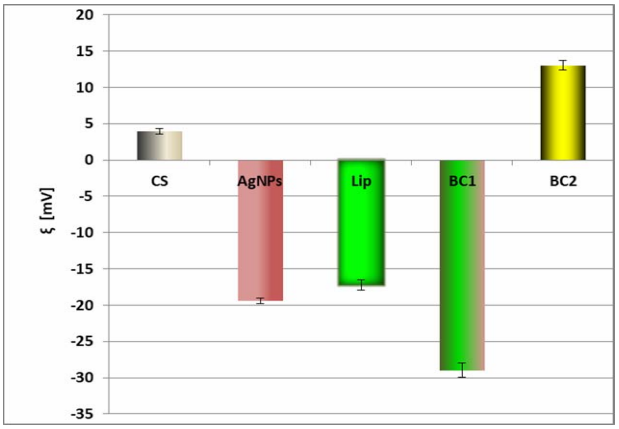

Fig. 5 – Zeta potential values of the samples (the results are reported on the basis of mean ± SD).

3.4. MORPHOLOGICAL CHARACTERIZATION OF THE MATERIALS BASED ON BIOGENIC NANOSILVER

SEM analysis of the bioreduced silver (*E. caryophyllata*-generated AgNPs) proved the synthesis of silver spherical nanoscaled particles (see Fig. 2, inset) with an average size less than 100 nm. Biosilver loading in bio-inspired lipid membranes generated two types of spherical-shaped hybrid colloidal materials (Figures 6(a) and 6(b)) with a predominantly mean size of 100 nm for BC1, and 125 nm for BC2.

It is noticed a tendency to aggregate in the case of BC2 particles (as compared to BC1) due to the presence of chitosan in its composition, which acts as a natural glue. The SEM results are in agreement with zeta potential measurements.

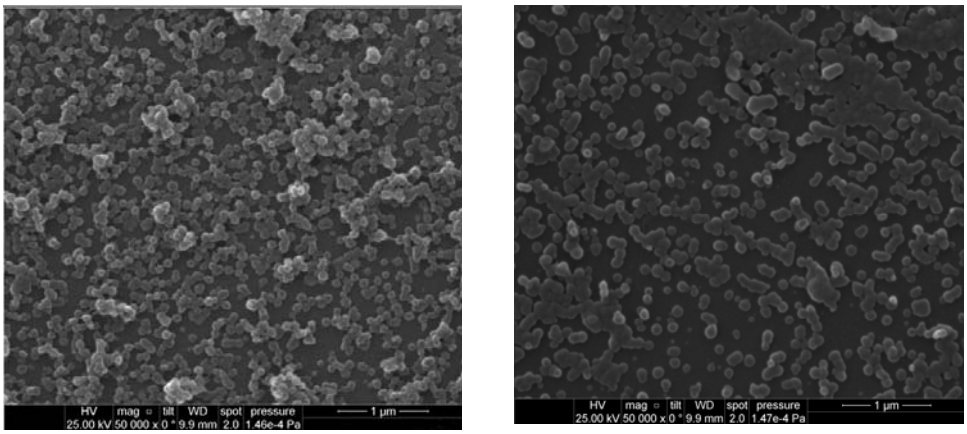

(a) BC1 **(b) BC2**

Fig. 6 – SEM images of the obtained hybrid colloidal materials BC1 (a) and BC2 (b).

3.5. EVALUATION OF THE BIO-ACTIVITIES OF THE BIO-BASED MATERIALS

The antioxidant activity of the samples was tested through chemiluminescence technique, by subjecting the samples to an *in vitro* oxidative stress induced by free radicals generated by H_2O_2 in alkaline medium; the values of AA% was calculated using the equation (2). All the prepared specimens exhibited antioxidant properties (Fig. 7), but only the silver-based materials have been shown to have high antioxidant activity: 90.2% for AgNPs, 97.2% for BC1, and 99.1% for BC2 due to the existence of natural antioxidant phyto-biomolecules on the surface of AgNPs acting as capping and stabilizing agents. The BC2 biohybrids proved to be most potent free radicals scavengers than BC1 due to the presence of chitosan, a natural–derived antioxidant and antimicrobial polysaccharide [15, 30], in their composition.

Viability of L929 and HT-29 cells incubated with the developed AgNPs and biocomposites BC1 and BC2 was assessed by MTS assay. The silver-based materials were used in a concentration range of 0÷14.4 µg/ml, related to AgNPs content. It could be noticed that biosynthesized AgNPs inhibited cells growth in a dose-dependent manner (Fig. 8), with an IC_{50} value of 3.03 µg/ml for L929 cells, and 2.7 µg/ml for HT-29 cells. Compared to AgNPs, the obtained biocomposites BC1 and BC2 proved to be less toxic at the concentrations tested. For the obtained silver-based materials, the safe concentration range assuring a viability ≥ 90% for L929 cells (indicating the biocompatibility of the samples), is 0÷1.8 µg/ml for AgNPs, while for BC1 and BC2 is 0÷3.6 µg/ml (related to AgNPs content). As observed in Fig. 8, at the above mentioned concentration ranges, the developed biocomposites

showed more toxicity to HT-29 cancer cells, and no toxicity to healthy cells. The biocomposite BC2 proved to be less toxic than BC1, due to the presence of chitosan in its composition. Moreover, as compared to BC1, the biocomposite BC2 proved to be more harmful against HT-29 cancer cells with no toxicity against L929 healthy cells, at an optimal AgNPs content of 1.8 μg/ml. In Table 2 are presented, if determined, IC_{50} values for the silver-based samples tested. Thus, the IC_{50} value for BC1 was calculated only for the L929 cells and was 11.7 μg/ml (related to silver content in its composition). Therefore, the lipid and chitosan coats played a key role to improve biocompatibility of the prepared silver nanoparticles, so higher content of silver could be therefore safely used in biomedical applications.

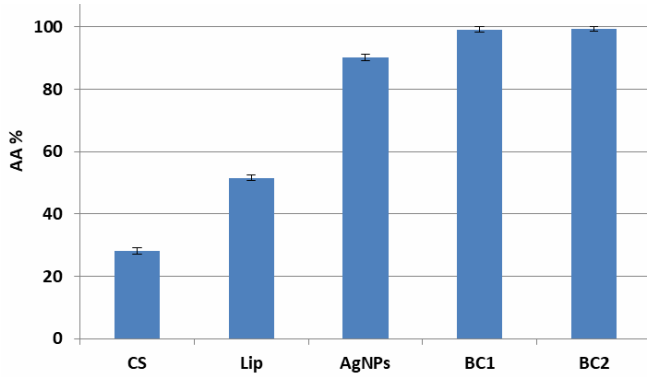

Fig. 7 – The antioxidant activity of the biosynthesized materials and their building blocks. The data are presented as mean ± SD.

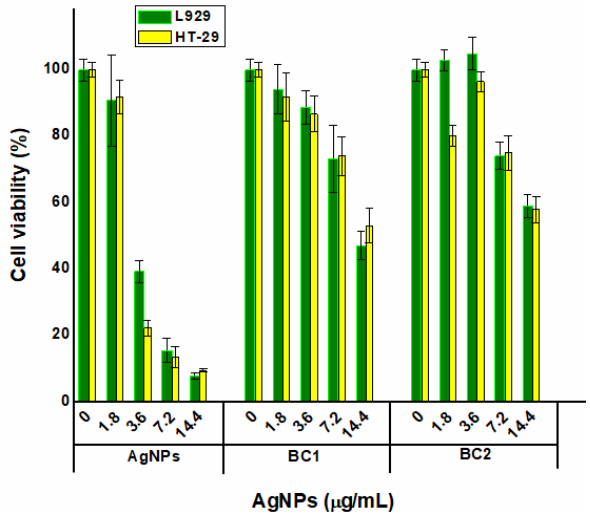

Fig. 8 – Cell viability of L929 and HT-29 cells incubated with different concentrations of the silver-based samples, for 24 h. The results are presented as mean ± SD.

Haemolysis was used to assess the biocompatibility of the biohybrids. Less than 5% haemolysis is considered as non-toxic according to the ASTM F 756-00 standard [23]. In Table 2 are also presented the percentage of haemolysis of the silver-based samples tested at their highest concentration. Only AgNPs alone showed haemolytic capacity. However, for the two biohybrids BC1 and BC2, no haemolysis was detected. It could be noticed the role played by chitosan and artificial lipid bilayers in reducing the toxicity of "green" synthesized AgNPs.

Table 2

The inhibitory concentration at 50% (IC50) and haemolysis percentage generated after treating the cells with the developed silver-loaded materials

Sample	IC_{50} L929 (µg/ml)*	IC_{50} HT-29 (µg/ml)*	Haemolysis** (%)
AgNPs	3.03 ± 0.209	2.7 ± 0.11	89.51 ± 7.4
BC1	11.7 ± 0.15	ND	1.94 ±0.38
BC2	ND	ND	2.13 ± 1.10

* *The values represent the silver content in the samples.*
** *Haemolysis was tested at the highest concentration of the silver-containing samples.*

The materials developed in this study presented low cytotoxicity as compared to our previous study [10]. Thus, a content of AgNPs 7.5 times higher could be safely used in biocomposites based on chitosan BC2 than in biohybrids obtained from soybean lecithin. These results could be explained by the presence of DPPC and chitosan in the structure of biocomposites.

4. CONCLUSIONS

This paper described an original *bottom*-up eco-design of novel nanocomposite materials based on chlorophyll-labeled biomimetic membranes, nanobiosilver and chitosan. Silver nanoparticles were *green* synthesized using the aqueous extract of *Eugenia caryophyllata* buds that acted both as reducing and capping agent. Through its spectral signatures (on UV-Vis absorption and fluorescence emission spectra), chlorophyll *a* inserted in artificial cell membranes offered useful information regarding the formation of biocomposites.

SEM images showed the nano-scaled dimension and (quasi-)spherical morphology of the developed silver-based materials. The prepared biocomposites exhibited different bio-activities due to the differences in their composition. The two obtained hybrid colloidal materials showed strong antioxidant properties, and also anti-proliferative activity against adenocarcinoma HT-29 cells and no toxicity to normal cells in a dose-dependent manner. The lipid and chitosan wrapping of *green* AgNPs improved the bioperformances of bionanosilver. Thus, biocompatibility of the prepared silver nanoparticles was enhanced, so higher content of silver could be therefore safely used in various bio-applications. Moreover, the biocomposite

containing chitosan proved to be more toxic against HT-29 cancer cells with no toxicity against L929 healthy cells, at an optimal concentration corresponding to a silver content of 1.8 μg/ml.

This research study opens a new perspective to develop new silver-based nanomaterials with great potential in colon cancer therapy.

Acknowledgements. The present study was supported by the Project No. 40/2019 (IUCN_Dubna Order no. 397/27.05.2019) of JINR-Romania (University of Bucharest, Faculty of Physics) collaboration (Theme No. 04-4-1121-2015/2020). M. Bacalum acknowledges the financial support of the Romanian National Authority for Research and Innovation (PN 18 09 02 02/2018, PN 19 06 02 03/2019, PN-III-P1-1.2-PCCDI-2017-0010/74PCCDI/2018). The authors thank to Anca Bonciu from University of Bucharest, Faculty of Physics (Bucharest, Romania) for performing SEM images.

REFERENCES

1. M. E. Barbinta-Patrascu, N. Badea, M. Constantin, C. Ungureanu, C. Nichita, S. M. Iordache, A. Vlad, S. Antohe, Rom. J. Phys. **63**(5–6), 702 (2018).
2. A. Popa, M. Stan, D. Toloman, S. A. Porav, R. Stefan, D. C. Vodnar, T. D. Silipas, Rom. J. Phys. **63**(5–6), 609 (2018).
3. G. Prasannaraj, S. V. Sahi, G.Benelli, P. Venkatachalam, J. Clust. Sci. **28**(4), 2349–2367 (2017).
4. M. E. Barbinta-Patrascu, C. Ungureanu, I.-R. Suica-Bunghez, A.-M. Iordache, S. Milenković Petrović, A. Ispas, I. Zgura, J. Optoelectron. Adv. Mat. **20**(9–10), 551–557 (2018).
5. S. Some, I. K. Sen, A. Mandal, T. Aslan, Y. Ustun, E. Ş. Yilmaz, A. Katı, A. Demirbas, A. K. Mandal, I. Ocsoy, Mater. Res. Express **6**(1), 012001 (2019).
6. A. J. Kora, R. B. Sashidhar, Arabian J. Chem. **11**, 313–323 (2018).
7. S. Kumar, M. Nehra, N.Dilbaghi, G. Marrazza, A. A. Hassan, K.-H. Kim, J. Controlled Release **294**, 131–153 (2019).
8. N. Nasr, M. H. Sayyad, J. Optoelectron. Adv. Mat. **20**(11–12), 618–623 (2018).
9. S. Gajbhiye, S. Sakharwade, J.Cosm.Derma.Sci.Appl. **6**, 48–53 (2016).
10. M. E. Barbinta-Patrascu, N. Badea, M. Bacalum, C. Ungureanu, I. R. Suica-Bunghez, S. M. Iordache, C. Pirvu, I. Zgura, V. A. Maraloiu, Mat. Sci. Eng. C **101**, 120–137 (2019).
11. M. E. Barbinta-Patrascu, M. Constantin, N. Badea, C. Ungureanu, S. M. Iordache, V. Purcar, S. Antohe, Rom. J. Phys. **64**(3–4), 701 (2019).
12. M. E. Barbinta-Patrascu, N. Badea, C. Ungureanu, S. M. Iordache, M. Constantin, V. Purcar, C. Pirvu, I. Rau, J. Nanomater. **2017**, 4214017 (2017).
13. D. F. Cortés-Rojas, C. R. Fernandes de Souza, W. P. Oliveira, Asian Pac. J. Trop. Biomed. **4**, 90–96 (2014).
14. M.E. Barbinta-Patrascu, N. Badea, C. Ungureanu, C. Pirvu, V. Iftimie, S. Antohe, Rom. Rep. Phys. **69**, 604 (2017)
15. M. E. Barbinta-Patrascu, N. Badea, C. Pirvu, M. Bacalum, C. Ungureanu, P. L. Nadejde, C. Ion, I. Rau, Mat. Sci. Eng. C **69**, 922–932 (2016).
16. Y. Jia, Y. Q. Hu, Y. X. Zhu, L. Che, Q. Y. Shen, J. X. Zhang, X. H. Li, Carbohydr. Polym. **83**, 1153–1161 (2011).
17. H. Liu, C. Wang, C. Li, Y. Qin, Z. Wang, F. Yang, Z. Li, J. Wang, RSC Adv. **8**, 7533–7549 (2018).
18. H. H. Strain, W. A. Svec, *The chlorophylls* (ed. L. P. Vernon and G. R Seely), Academic Press, New York, 1966, p. 21–66.
19. M. E Barbinta-Patrascu, C. Ungureanu, S. M. Iordache, A. M. Iordache, I. R. Bunghez, M. Ghiurea, N. Badea, R. C. Fierascu, I. Stamatin, Mat. Sci. Eng. C **39**, 177–185 (2014).

20. M. E. Barbinta-Patrascu, I. R. Bunghez, S. M. Iordache, N. Badea, R. C. Fierascu, R M. Ion, J. Nanosci. Nanotechnol. **13**(3), 2051–2060 (2013).
21. M. E. Barbinta-Patrascu, S. M. Iordache, A. M. Iordache, N. Badea, C. Ungureanu, Beilstein J. Nanotechnol. **5**, 2316–2325 (2014).
22. I. Lacatusu, N. Badea, G. Badea, O. Oprea, M. A. Mihaila, D. A. Kaya, R. Stan, A. Meghea, Mat. Sci. Eng. C **56**, 88–94 (2015).
23. ASTM, *F 756-00 – Standard Practice for Assessment of Hemolytic Properties of Materials*, West Conshohocken, Pa, USA: American Society for Testing of Materials, 2000.
24. M. Bacalum, M. Radu, Int. J. Pept. Res. Ther. **21**(1), 47–55 (2015).
25. A. J. Kora, S. R. Beedu, A. Jayaraman, Org. Med. Chem. Lett. **2**, 1–10 (2012).
26. M. E. Barbinta-Patrascu, L. Tugulea, A. Meghea, A. Popescu, Optoelectron. Adv. Mat. **2**(2), 113–116 (2008).
27. W. F. Falco, A. M. Queiroz, J. Fernandes, E. R. Botero, E. A. Falcão, F.E.G. Guimarães, J.-C. M'Peko, S. L. Oliveira, I. Colbeck, A. R. L. Caires, J. Photochem. Photobiol. A **299**, 203–209 (2015).
28. J. Lakowicz, C. Geddes, I. Gryczynski, J. Malicka, Z. Gryczynski, K. Aslan, J. Lukomska, E. Matveeva, J. Zhang, R. Badugu, J. Huang, J. Fluorescence **14**(4), 425–441 (2004).
29. P. R. Mishra, L. Al Shaal, R. H. Müller, C. M. Keck, Int. J. Pharm. **371**, 182–189 (2009).
30. M. Dasha, F. Chiellini, R. M. Ottenbrite, E. Chiellini, Prog. Polym. Sci. **36**, 981–1014 (2011).